HAL
open science

Scaling and universality in the kinetic smoothening of interfaces: Application to the analysis of the relaxation of rough vicinal steps of an oxide surface

Thi Thu Thuy Nguyen, Daniel Bonamy, Laurent Phan Vam, Jacques Cousty, Luc Barbier

To cite this version:

Thi Thu Thuy Nguyen, Daniel Bonamy, Laurent Phan Vam, Jacques Cousty, Luc Barbier. Scaling and universality in the kinetic smoothening of interfaces: Application to the analysis of the relaxation of rough vicinal steps of an oxide surface. EPL - Europhysics Letters, 2010, 89 (6), pp.60005. 10.1209/0295-5075/89/60005 . hal-00375416v1

HAL Id: hal-00375416

https://hal.science/hal-00375416v1

Submitted on 14 Apr 2009 (v1), last revised 24 Aug 2010 (v2)

HAL is a multi-disciplinary open access archive for the deposit and dissemination of scientific research documents, whether they are published or not. The documents may come from teaching and research institutions in France or abroad, or from public or private research centers.

L'archive ouverte pluridisciplinaire **HAL**, est destinée au dépôt et à la diffusion de documents scientifiques de niveau recherche, publiés ou non, émanant des établissements d'enseignement et de recherche français ou étrangers, des laboratoires publics ou privés.

Scaling law for out-of-equilibrium smoothening of rough vicinal steps. Application to oxide surfaces during annealing

T.T.T. Nguyen,[1] D. Bonamy,[1] L. Phan Van,[1] J. Cousty,[1] and L. Barbier[1]

[1] *CEA, IRAMIS, SPCSI, F-91191 Gif sur Yvette, France*

(Dated: April 14, 2009)

Langevin formalism approach is used to derive analytically the time evolution of the correlation function of steps in vicinal surfaces during annealing back to thermal equilibrium. A new generic scaling form is obtained for smoothening far-from-equilibrium one dimension objects. This approach allows interpreting a series of AFM images of sapphire surfaces showing the thermal evolution of initially rough step edges. From this analyse, we deduce that the step smoothening for $(1, \bar{1}, 0, 2)$ vicinal surfaces is governed by surface diffusion via a detachment-attachment mechanism during annealing at 1273K ($\simeq 0.6T_{melting}$).

PACS numbers: 05.70.Np;64.60.Ht;68.35.Ct;68.37.-d;

Understanding how the competition between elasticity and disorder sets the morphological dynamics of interfaces is a central theme of current research in statistical physics. It appears in the context of surface growth [1, 2], thermal fluctuations of vicinal surfaces [3], domain wall motion in magnetic [4] or ferroelectric [5] materials, flux lines in superconductors [6], cracks in solids [7], among other realizations. One of the most striking results in this field is the observation of spatio-temporal scale-invariant features characterized by exponents remarkably similar in systems with no apparent connection between them (see [1] for a review). Guided by this universality, it was then suggested that the interface motion should be described by the simplest possible Langevin equations compatible with the symmetries of the problem [8].

This Langevin formalism was successfully applied to describe the fluctuations of crystal surfaces at thermal equilibrium. This approach was used to interpret the spatial and temporal correlation functions measured from STM images [3, 9, 10, 11] and allowed to measure quantities as e.g. the elementary kink energy [9, 10] or atomic diffusion energies [3, 11]. This is central for understanding and predicting the stability of surfaces/interfaces, and therefore the stability of associated nanostructure together with their physical and reactivity properties.

Beyond thermal equilibrium studies, one may observe the evolution towards stability of initially flat (low T equilibrated surface below its roughening transition T_R [12]) or rough surfaces (after initial preparation, high T annealing, growth or other surface processes). Such situations are the most common and in the following we show that the Langevin formalism approach may be extended to give interpretation of these very far from equilibrium states, leading to the determination of physical parameters (surface tension, relaxation time constant). For illustration of the method we applied this Langevin formalism to the experimental study of a vicinal surface of oxides. Such surfaces are difficult to equilibrates as long annealing at high temperature are needed during which it is difficult to maintain the stoichiometry. In addition, very few studies, except for scarcely AFM investigations [13], concern the surfaces of insulating oxides. To follow the smoothening of the atomic steps, we derive analytically the time evolution of the spatial correlation function of the step position. This one is found to exhibit a generic form that generalizes the Family-Viseck scaling classically used to describe roughening of initially flat interfaces. The predictions are then compared to experimental results on vicinal $(1, \bar{1}, 0, 2)$-sapphire surfaces. The time evolution of the step height correlation function can be perfectly reproduced and values of both the step stiffness and the atom hopping rate are deduced.

Langevin equation of the out-of-equilibrium interface dynamics – Specifically, we consider a vicinal surface such as the one depicted in Fig. 1. The vicinal angle being small, the step density is low allowing to neglect the step-step interaction and allowing the use of a 1-d model. The morphological evolution is characterized by the series displacement $h(m, y, t)$ of the step numbered m (for an ideally ordered system, $x = mL$, L being the nominal step-step distance) at time t and location y. Within the capillary wave model, the Hamiltonian H of an isolated step such as the ones represented on Fig. 1 can be written [14]:

$$H = \int \frac{\eta}{2} \left(\frac{\partial h}{\partial y} \right)^2 dy \tag{1}$$

where η refers to the stiffness parallel to the step edge. In the Langevin formalism, the step profile is assumed to relax locally to minimize its energy. The back force depends on the diffusion processes. Without matter conservation, i.e. for evaporation-condensation of atoms at isolate steps, this force is simply proportional to the energy gradient $\delta H/\delta h(y)$, and the 1D Langevin equation takes the form of an Edwards-Wilkinson equation [9, 10]:

$$\frac{\partial h(y)}{\partial t} = \frac{\eta \Gamma}{kT} \frac{\partial^2 h}{\partial y^2} + \xi(y, t) \tag{2}$$

where Γ denotes the atom hopping rate and $\xi(y, t)$ is a noise term allowing for thermal fluctuations. This noise is

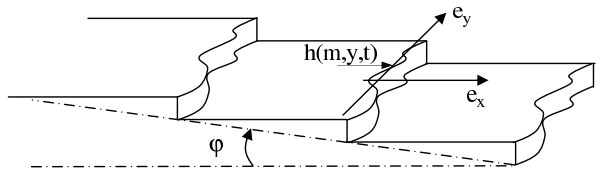

FIG. 1: Sketch and notations introduced in the text: The frame $\{\vec{e}_x, \vec{e}_y\}$ is chosen so that $\vec{e}_x$ and $\vec{e}_y$ are perpendicular and parallel to the mean step edges respectively, φ denotes the angle between terrace and the mean surface plane.

uncorrelated in space and time and its correlation function can be written:

$$\langle \xi(y',t')\xi(y,t)\rangle = 2\Gamma\delta(y'-y)\delta(t'-t) \tag{3}$$

Note that the very same constant Γ appears in Eqs. 2 and 3 making the principle of energy partition at thermal equilibrium satisfied.

To characterize the dynamics of a fluctuating interface $h(y,t)$, one usually computes the time evolution of the spatial correlation function $G(\Delta y,t) = \left\langle (h(y+\Delta y,t)-h(y,t))^2\right\rangle$. This function can be analytically derived from Eq. 2. Let us first discretize the step profile: $h_{n_y}(t) = h(y = n_y a_y, t)$ ($n_y = \{-N/2, ..., N/2-1\}$ with a_y the lattice constant) and call $\tilde{h}_q(t) = (1/\sqrt{N})\sum_{n_y} h_{n_y}(t) e^{-2\pi i q \frac{n_y}{N}}$ the $y-$ discrete Fourier transform of h. $\tilde{\eta}_q(t)$ is similarly defined. Then Eq. 2 writes:

$$\frac{\partial \tilde{h}_q(t)}{\partial t} = -\frac{4\pi^2}{a_y^2 N^2}\nu q \tilde{h}_q(t) + \tilde{\eta}_q(t) \tag{4}$$

with $\nu = \eta\Gamma/kT$. Its solution is given by:

$$\tilde{h}_q(t) = e^{-\frac{4\pi^2}{a_y^2N^2}\nu q^2 t}\left(\tilde{h}_q(0) + \int_0^t \tilde{\eta}_q(u) e^{\frac{4\pi^2}{a_y^2N^2}\nu q^2 u} du\right) \tag{5}$$

where $\tilde{h}_q(0)$ is the y-Fourier transform of the step profile $h(y,0)$ at time $t=0$. Back into real space, the step profile can be computed, and the complete time evolution of the spatial correlation function $G(\Delta y,t)$ is deduced:

$$G(\Delta y,t) = \frac{2\Gamma a_y N}{\pi^2\nu}\sum_{q=1}^{N/2}\frac{1}{q^2}\left(1-e^{-\frac{8\pi^2}{a_y^2N^2}\nu q^2 t}\right)\left(1-\cos(2\pi\Delta y\frac{q}{a_yN})\right) + \frac{4}{N}\sum_{q=1}^{N/2}|\tilde{h}_q|^2(0)e^{-\frac{8\pi^2}{a_y^2N^2}\nu q^2 t}\left(1-\cos(2\pi\Delta y\frac{q}{a_yN})\right) \tag{6}$$

The form of G can now be discussed. It is written as the sum of two terms $G = G^{rough}(\Delta y,t) + G^{smooth}(\Delta y,t)$. The first term $G^{rough}(\Delta y,t)$ describes the roughening of an initially flat step under the action of the thermal noise ξ. This situation has been extensively studied in the context of interface roughening problems and $G^{rough}(\Delta y,t)$ was shown to take the specific form, so-called Family-Viseck form[15]:

$$G^{rough}(\Delta y,t) = t^{2\beta} f(\Delta y/t^{1/z})$$
$$where \quad f(u) = \begin{cases} f_0(u/u_0)^{2\zeta} & \text{if u}\ll u_0 \\ f_0 & \text{if u}\gg u_0 \end{cases} \tag{7}$$

Where the exponents $\zeta = 1/2$, $\beta = 1/4$ and $z = \zeta/\beta = 2$ refer to the roughness, growth and dynamic exponents, respectively. The two parameters f_0 and u_0 can be related to the two parameters ν and Γ of the Langevin equation (Eq. 2): $f_0 \simeq 1.5\Gamma\nu^{-1/2}$ and $u_0 \simeq 1.7\nu^{1/2}$. The second term $G^{smooth}(\Delta y,t)$ of Eq. 6 describes the smoothening of the initial profile $h(y,t=0)$ because of the line tension ν in absence of thermal fluctuations. Without loss of generality, let us consider an initially rough uncorrelated profile with zero average and variance set to σ_0^2: $\langle h(y,t=0)h(y',t=0)\rangle = \sigma_0^2\delta(y-y')$. G^{smooth} is then given by $G^{smooth} = (2\sigma_0^2/N)\sum_q e^{-\frac{8\pi^2}{a_y^2N^2}\nu q^2 t}(1-\cos(2\pi\Delta y(q/a_yN)))$ which takes the new generic form (Note the minus sign of the exponents and the abscence of the ζ exponent):

$$G^{smooth}(\Delta y,t) = t^{-2\beta} g(\Delta y/t^{1/z})$$
$$where \quad g(v) = \begin{cases} g_0(v/v_0)^2 & \text{if v}\ll v_0 \\ g_0 & \text{if v}\gg v_0 \end{cases} \tag{8}$$

Where the two parameters g_0 and v_0 can be related to the two parameters ν and Γ of the Langevin equation (Eq. 2): $g_0 \simeq 0.2\sigma_0^2 a_y \nu^{-1/2}$ and $v_0 \simeq 2.9\nu^{1/2}$.

From the forms of $G^{rough}(\Delta y,t)$ and $G^{smooth}(\Delta y,t)$, - given by Eq. 7 and Eq. 8 respectively -, one can deduce the global behaviour of $G(\Delta y,t)$. This is sketched in Fig. 2. Depending on the time t, two cases can be distinguished:

- For small time, i.e. for $t \ll \sigma_0^2 a_y/\Gamma$), the variation of the spatial correlation function $G(\Delta y,t)$ can be decomposed into three regimes. At small scales, thermal equilibrium is reached and $G^{rough}(\Delta y,t)$ dominates $G(\Delta y,t)$. At medium and large scales, $G(\Delta y,t)$ results from the smoothening of the initial roughness and $G^{smooth}(\Delta y,t)$ dominates:

$$\begin{array}{ll} \Delta y \ll \lambda(t) & G(\Delta y,t) \approx (\Gamma/\nu)\Delta y \\ \lambda(t) \ll \Delta y \ll \xi(t) & G(\Delta y,t) \approx 0.025\sigma_0^2 a_y(\nu t)^{-3/2}\Delta y^2 \\ \Delta y \gg \xi(t) & G(\Delta y,t) \approx 0.2\sigma_0^2 a_y(\nu t)^{-1/2} \end{array} \tag{9}$$

  with $\lambda(t) \approx \frac{\Gamma}{\nu\sigma_0^2 a_y^{1/2}}(\nu t)^{3/2}$ and $\xi(t) \approx (\nu t)^{1/2}$.

- For large time, i.e. for $t \gg \sigma_0^2 a_y/\Gamma$, the influence of the initial conditions $h(y,t=0)$ is not seen anymore. The spatial correlation function $G(\Delta y,t)$ is

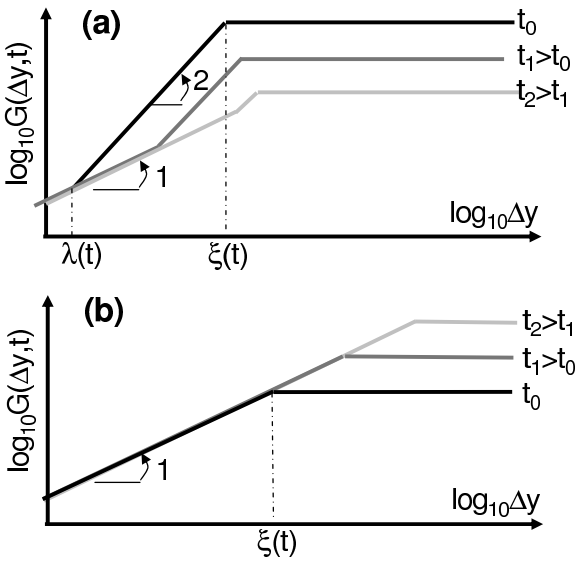

FIG. 2: Schematic illustration of the spatial correlation function describing the time evolution of a step profile starting from an initially uncorrelated rough profile $h(y, t = 0)$ with zero average and σ_0^2 variance. (a) Smoothing regime observed for small times (see Eq. 9). (b) Roughening regime observed at large times (see Eq. 11).

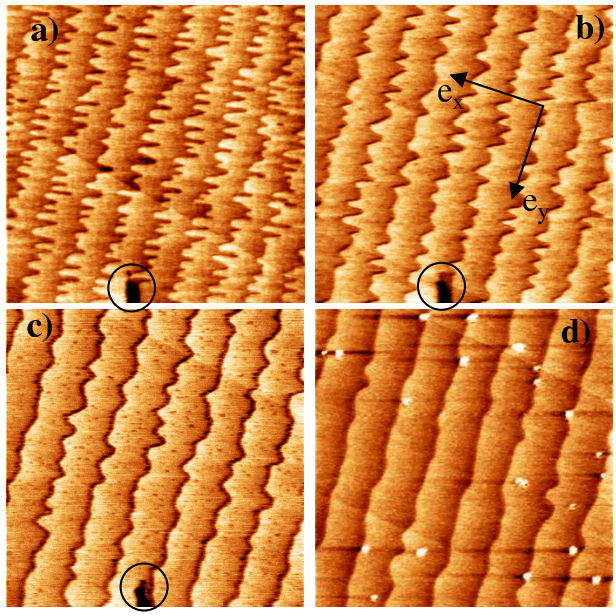

FIG. 3: 5×5 μm^2 contact mode AFM images of the topography of a $(1\bar{1}02)$ vicinal surface of sapphire after a) 5400s, b) 12600s, c) 23400s et d) 37800s of annealing at 1273K. The axis e_x coincides with the $[\bar{1}, 1, 0, 1]$ direction. Note the defect (black circles) in (a)-(c) that proves the accurate repositioning of the AFM tip between two successive annealing processes.

then given by $G^{rough}(\Delta y, t)$ for all Δy with two power-law regimes:

$$\begin{aligned} \Delta y \ll \xi(t) \qquad & G(\Delta y, t) \approx (\Gamma/\nu)\Delta y \\ \Delta y \gg \xi(t) \qquad & G(\Delta y, t) \approx 1.5(\Gamma/\nu)(\nu t)^{1/2} \end{aligned} \tag{10}$$

with $\xi(t) \approx (\nu t)^{1/2}$.

Experiments – This can now be confronted to observations performed on the smoothening dynamics of vicinal surfaces in oxide surfaces. The samples studied here consist in square slabs of sapphire (Le Rubis S.A., 10mm side, 0.2mm thick) with a surface oriented close to the $(1, \bar{1}, 0, 2)$ plane (misorientation $\simeq 0.06°$). They present important technological interest as substrate for nanostructures, magnetic thin layers or giant magnetoresistance devices [17]. These surfaces are first chemo-mechanically polished to an optical grade, and carefully cleaned in an ultrasonic bath. As a result, one gets a rough out-of-equilibrium vicinal surface. A series of annealing in air (essential to maintain the surface stoichiometry) at constant temperature for increasing cumulated durations are then performed in an oven. After each annealing phase, the sample is cooled down to room temperature (cooling rate of 30K/min) and the vicinal surface is imaged via a Molecular Imaging Pico+ AFM in contact mode with gold coated Si_3N_4 cantilevers (0.58 N/m stiffness). Special attention was paid so that our setup allows for an accurate and reproducible positioning of the AFM tip onto the surface and allows to image *the very same* area after each annealing treatment (see e.g. [16] for details).

Depending on the temperature T, two regimes can be observed. At low temperature $973\,\mathrm{K} \leq T \leq 1173\,\mathrm{K}$, the evolution of the surface morphology is governed by the coarsening of 2D islands through anisotropic Oswald ripening during the experimental time. This regime was studied in a previous paper [16] and will not be discussed thereafter. At high temperature $1173\,\mathrm{K} \leq T \leq 1473\,\mathrm{K}$, all the islands shrink up and overhangs in steps disappear rapidly, in less than one hour for $T = 1173\,\mathrm{K}$. After this initial regime, the evolution of the surface morphology is governed by the smoothening of the vicinal steps that can be described by Eq. 2.

Typical AFM images of the vicinal surface taken after increasing cumulated annealing durations are presented in Fig. 3. The meandering lines are the steps defining the terraces. Contrast enhancement, image analysis and edge detection allow measuring $h(m, y, t)$ and then computing $G(\Delta y, t) = \langle (h(m, y + \Delta y, t) - h(m, y, t))^2 \rangle_{m,y}$ where the average has been performed over all edges of a given image to improve the statistics. Note that the mean distance between two successive steps remains constant and pretty large ($\simeq 750$ nm). This suggests that the morphological fluctuations of a given step is independent from the neighbouring ones, as assumed in the Langevin description proposed in Eq. 2.

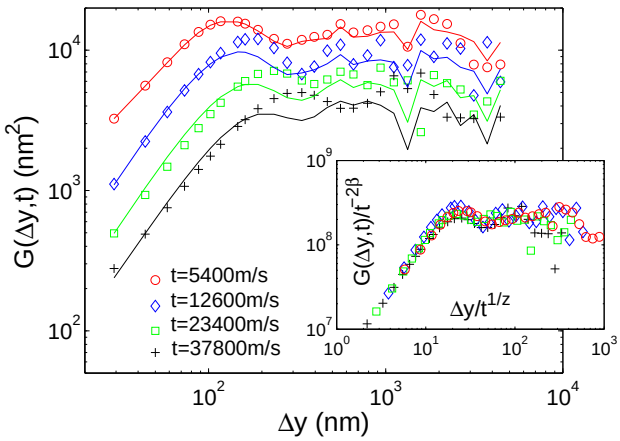

FIG. 4: spatial correlation function $G(\Delta y, t)$ of the step edges of the $(1\bar{1}02)$ alumina surface for various cumulative durations t of annealing at $T = 1273K$ K. The axis are logarithmic. The symbols correspond to experiments while the continuous lines corresponds to the analytical expression given Eq. 6 with $\nu = 7.2 \times 10^{-2}\,\mathrm{nm}^2.\mathrm{s}$ and $\Gamma = 5.3 \times 10^{-2}\,\mathrm{nm}^3.\mathrm{s}$

The experimental correlation functions are plotted in Fig. 4. They exhibit the scaling given by Eq. 8 (Inset of Fig. 4) expected in the far-from-equilibrium smoothening regime. Initial conditions are set by the image taken at $t_0 = 5400\,\mathrm{s}$, the step profiles of which give the initial Fourier amplitudes $|\tilde{h}_q|^2(t_0)$. The subsequent experimental correlation functions are then fitted successfully using the analytical expression (Eq. 6) (continuous lines in Fig. 4). This provides a severe test in favour of the present extension of Langevin formalism to far out-of-equilibrium systems.

Note that the linear regime expected at thermal equilibrium is not apparent after more than 10h annealing. From the fitted values $\nu = 7.2 \times 10^{-2}\,\mathrm{nm}^2.\mathrm{s}^{-1}$ and $\Gamma = 5.3 \times 10^{-2}\,\mathrm{nm}^3.\mathrm{s}^{-1}$ (Fig. 4), the initial roughness $\sigma_0 \simeq 100\,\mathrm{nm}$, and from the pixel size $a_y = 14.6\,\mathrm{nm}$ of the images, one estimates the time τ_{eq} to pass from the out-of-equilibrium smoothening regime to the equilibrium roughening regime: $\tau_{eq} = \sigma_0^2 a_y/\Gamma \simeq 32$ days. This makes this last regime difficult to observe experimentally and emphasizes all the importance of the out-of-equilibirum extension of the Langevin formalism to determine the physical parameters in oxyde surfaces.

In summary, we used here Langevin formalism to derive analytically the time evolution of the spatial correlation function of initially rough steps of vicinal surfaces relaxing toward thermal equilibrium. Far from equilibrium, this one is found to exhibit a generic scaling (Eq. 8) independent of the details of the considered system provided that the dynamics remains linear. On the other hand, the value of the exponents $\{\beta, z\}$ depends whether the dynamics and the noise are conservative or not (see [1] for review). In particular they are found to be $\{\beta = 1/8, z = 4\}$ for conservative dynamics and noise that is expected at the onset of active diffusion [3] and commonly observed in metallic surfaces [11]. Such a regime is surprisingly not observed for the $(1, \bar{1}, 0, 2)$ sapphire surfaces investigated here. Two origins of these non-conservative processes can be invoked: (i) The channelled structure of terraces which was shown to influence the Ostwald ripening at low T [16]; These channels parallel to $[\bar{1}, 1, 0, 1]$ and roughly perpendicular to the step edge makes the mobility along the step edge difficult. As a result, atoms emitted from the step are diffusing on the terraces then captured on the same step at a different site (detachment/attachment mechanism); (ii) The exchange of oxygen atoms, during annealing, with the surrounding atmosphere, evidenced by a different morphology of terraces after UHV annealing at 1273K [18]. This makes the extension of the present work to the various conservative cases and to higher dimensions of high interest. Work in this direction is under progress.

The authors thank the invaluable technical support of C. Lubin, F. Thoyer and S. Foucquart. Interesting discussions with S. Bustingorry are also gratefully acknowledged.

[1] A. L. Barbarasi and H. E. Stanley, *Fractal concepts in surface growth* (Cambridge Univ. Press,Cambridge, 1995).
[2] A. Pimpinelli, V. Tonchev, A. Videcoq and M. Vladimirova, Phys. Rev. Lett. **88**, 206103 (2002);
[3] E. Le Goff, L. Barbier and B. Salanon, Surf. Sci. **531**, 337 (2003)
[4] A. J. Bray, Adv. Phys. **43**, 357 (1994).
[5] T. Nattermann and S. Scheidl, Adv. Phys. **49**, 607 (2000)
[6] G. Blatter et al., Rev. Mod. Phys. **66**, 1125 (1994); S. Bustingorry, L. F. Cugliandolo and D. Dominguez, Phys. Rev. Lett. **96**, 027001 (2006)
[7] J. Schmittbuhl, S. Roux, J. P. Vilotte, and K. J. Maloy. Phys. Rev. Lett. **74**, 1787, (1995); L. Ponson, D. Bonamy, E. Bouchaud, Phys. Rev. Lett. **96**, 035506 (2006); L. Ponson, D. Bonamy, L. Barbier, Phys. Rev. B **74**, 184205 (2006).
[8] S. F. Edwards and D. R. Wilkinson, Proc. Roy. Acad. London, Ser. A **381**, 17 (1982); M. Kardar, G. Parisi, and Y.-C. Zhang, Phys. Rev. Lett. **56**, 889 (1986); T. Sun, H. Guo and M. Grant, Phys. Rev. A **40**, 6763 (1989); D.E. Wolf and J. Villain, Europhys. Lett. **13**, 389 (1990).
[9] L. Masson, L. Barbier, J. Cousty and B. Salanon, Surf. Sci. **317**, L1115 (1994); L. Barbier, L. Masson, J. Cousty and B. Salanon, Surface Science **345**, 197 (1996); E. Le Goff, L. Barbier, L. Masson and B. Salanon, Surf. Sci. **432**, 139 (1999).
[10] N. C. Bartelt, J. L. Goldberg, T. L. Einstein and E. Williams, Surf. Sci. **273**, 1 (1992).
[11] M Giesen, Prog. Surf. Sci. **68**, 1 (2001).
[12] J. Lapujoulade, Surf. Sci Rep. **20**, 191 (1994); A. Pimpinelli and J. Villain, *Physics of crystal growth*,

(Cambridge Univ. Press, Cambridge, 1998).
[13] C. Barth and M. Reichling, Nature **414**, 54 (2001); L. Pham-Van, O. Kurnosikov, J. Cousty, Surf. Sci. **411**, 263 (1998); W. Steurer et al., Surf. Sci. **601**, 4407 (2007).
[14] J. V. José, L. P. Kadanoff, S. Kirkpatrick and D. R. Nelson, Phys. Rev. B **16**, 1217 (1977); J. Villain, D. R. Grimpel and J. Lapujoulade, J. Phys. F **15**, 809 (1985).
[15] F. Family and T. Vicsek, *Dynamics of fractal surfaces* (World Scientific,1991).
[16] T.T.T. Nguyen et al. Surf. Sci. **602**, 3232 (2008).
[17] T. Fujii et al., J. Appl. Phys. **66**, 3168 (1989); W. Eerenstein, T. T. M. Palstra, S. S. Saxena and T. Hibma, Phys. Rev. Lett. **88**, 247204 (2002); A. V. Ramos et al., Phys. Rev. B **75**, 224421 (2007).
[18] T.T.T. Nguyen, PhD Thesis (2008).